Appendix N: Conditional, Time-Dependent Probabilities for Segmented Type-A Faults in the WGCEP UCERF 2

By Edward H. Field[1] and Vipin Gupta[2]

USGS Open File Report 2007-1437N
CGS Special Report 203N
SCEC Contribution #1138N
Version 1.0

2008

U.S. Department of the Interior
U.S. Geological Survey

California Department of Conservation
California Geological Survey

[1]U.S. Geological Survey, Pasadena, California
[2]University of Southern California, Los Angeles, California

U.S. Department of the Interior
DIRK KEMPTHORNE, Secretary

U.S. Geological Survey
Mark D. Myers, Director

State of California
ARNOLD SCHWARZENEGGER, Governor

The Resources Agency
MIKE CHRISMAN, Secretary for Resources

Department of Conservation
Bridgett Luther, Director

California Geological Survey
John G. Parrish, Ph.D., State Geologist

U.S. Geological Survey, Reston, Virginia 2008

For product and ordering information:
World Wide Web: http://www.usgs.gov/pubprod
Telephone: 1-888-ASK-USGS

For more information on the USGS—the Federal source for science about the Earth,
its natural and living resources, natural hazards, and the environment:
World Wide Web: http://www.usgs.gov
Telephone: 1-888-ASK-USGS

Suggested citation:
Field, E. H., and Gupta, V. 2008, Conditional, Time-dependent probabilities for segmented Type-A faults in the WGCEP UCERF 2, *Appendix N in* The Uniform California Earthquake Rupture Forecast, version 2 (UCERF 2): U.S. Geological Survey Open-File Report 2007-1437N and California Geological Survey Special Report 203N, 7 p. [http://pubs.usgs.gov/of/2007/1437/n/].

Appendix N

Conditional, Time-Dependent Probabilities for Segmented Type-A Faults in the WGCEP UCERF 2

Edward (Ned) Field & Vipin Gupta

Introduction

This appendix presents elastic-rebound-theory (ERT) motivated time-dependent probabilities, conditioned on the date of last earthquake, for the segmented type-A fault models of the 2007 Working Group on California Earthquake Probabilities (WGCEP). These probabilities are included as one option in the WGCEP's Uniform California Earthquake Rupture Forecast 2 (UCERF 2), with the other options being time-independent Poisson probabilities and an "Empirical" model based on observed seismicity rate changes. A more general discussion of the pros and cons of all methods for computing time-dependent probabilities, as well as the justification of those chosen for UCERF 2, are given in the main body of this report (and the "Empirical" model is also discussed in Appendix M). What this appendix addresses is the computation of conditional, time-dependent probabilities when both single- and multi-segment ruptures are included in the model.

Computing conditional probabilities is relatively straightforward when a fault is assumed to obey strict segmentation in the sense that no multi-segment ruptures occur (e.g., WGCEP (1988, 1990) or see Field (2007) for a review of all previous WGCEPs; from here we assume basic familiarity with conditional probability calculations). However, and as we'll see below, the calculation is not straightforward when multi-segment ruptures are included, in essence because we are attempting to apply a point-process model to a non point process.

The next section gives a review and evaluation of the single- and multi-segment rupture probability-calculation methods used in the most recent statewide forecast for California (WGCEP UCERF 1; Petersen et al., 2007). We then present results for the methodology adopted here for UCERF 2. We finish with a discussion of issues and possible alternative approaches that could be explored and perhaps applied in the future. A fault-by-fault comparison of UCERF 2 probabilities with those of previous studies is given in the main part of this report.

Time-Dependent Models Used Previously in UCERF 1

There were basically three difference approaches used for computing single- and multi-segment rupture probabilities in WGCEP UCERF 1:

a) The WGCEP (2003) approach for the San Francisco bay area faults

b) Time-Dependent Model 1 ("T-D Model 1", applied to the S. San Andreas Fault (SAF), and equivalent to their "T-D Model 3" in terms of the discussion here.

c) Time-Dependent Model 2 ("T-D Model 2", applied to the S. SAF).

(all other faults that had time-dependent probabilities in UCERF 1 had only single-segment ruptures). Each of these methodologies began with a moment-balanced long-term rate model and then applied some rules to obtain time-dependent probabilities based on dates of previous events and, in some cases, other information. By moment balanced we simply mean the model is consistent with fault slip rates. A question that will be evaluated here is whether these probability calculation rules can be applied repeatedly and indefinitely (e.g., as earthquakes occur in the future) without violating the long-term model or assumptions that went into the methodology.

WGCEP (2003) Methodology

The long-term rate model developed by the 2002 WGCEP resulted in a moment-balanced relative frequency of occurrence for each single and multi-segment rupture combination on each fault. A simplified example of the possible ruptures and their frequencies of occurrence for the Hayward/Rodgers-Creek fault are shown in Figure 1 (see the caption for details, and note that none of the simplifications influence the conclusions that will be drawn here). From the long-term rate of each rupture they had four different ways of getting time-dependent probabilities: a Brownian Passage Time (BPT) model, a BPT-step model, an Empirical model, and a Time-Predictable model. Again, a more general discussion of each of these models is included in the main part of this report, whereas here we focus on their procedure for computing conditional probabilities of single and multi-segment ruptures. The discussion here will be in the context of their BPT model, although the issues exemplified are applicable to the BPT-step and Time-Predictable models as well.

From the long-term rate of each rupture, conditional time-dependent probabilities for each rupture were computed as:

$$P(rup) = \sum_{segs\_in\_rup} P(seg)\frac{R(rup)}{R(seg)}\frac{\dot{M}o(seg)}{\sum_{segs\_in\_rup}\dot{M}o(seg)} \quad (1)$$

where "rup" and "seg" stand for rupture and segment, respectively, *P*() represents time-dependent probabilities, *R*() represents long-term event rates, $\dot{M}o()$ represents moment rate, and the summations are over all segments that participate in the particular rupture. P(seg) is computed from a Brownian Passage Time (BPT) model (e.g., Matthews et al., 2002) using the date of the last event on the segment and the average recurrence interval for the segment (one over the long-term rate of all ruptures involved in that segment). If the rates are low, such that they are approximately equal to Poisson probabilities (e.g., $P_{pois}() \approx R()$), then the above can be written as:

$$P(rup) \approx P_{pois}(rup)\frac{\sum_{seg\_in\_rup}\frac{P(seg)}{P_{pois}(seg)}\dot{M}o(seg)}{\sum_{seg\_in\_rup}\dot{M}o(seg)} \quad (2)$$

Thus, the time-dependent probability of the earthquake is simply the time-independent probability multiplied by a weight-averaged probability gain ($P(seg)/P_{pois}(seg)$) for the segments involved in that rupture, where the weights are the segment moment rates. Another way of describing the WGCEP (2003) approach is that they first compute the probability that each segment will rupture (assuming a BPT distribution) and then partition these probabilities among all ruptures that could be triggered by each segment.

Monte Carlo simulations were conducted to explore the implications of this model when applied over repeated earthquake cycles. Specifically, earthquake probabilities were computed at 1-year time intervals, ruptures were allowed to occur at random according to the probabilities for that year, dates of last events were updated on each relevant segment when an earthquake occurred, and probabilities were updated for the next year. This process was repeated until 20,000 events were sampled. Results for the simplified Hayward-Rodgers Creek example in Figure 1 are shown in Figure 2. The red lines show the assumed distribution of recurrence intervals on each segment (used in computing segment probabilities) and the gray bins represent the distribution of segment recurrence intervals actually "observed" from the simulation. Note that the simulations exhibit more short recurrence intervals than assumed in the original probability distribution for each segment. This arises from the fact that in the WGCEP (2003) methodology, the probability of a segment rupturing and taking its neighbor with it has nothing to do with when that neighbor last ruptured. Therefore, a segment can rupture one day by itself, and then rupture again the next day if triggered by its neighbor. While this behavior may indeed be desirable (i.e., accurately reflecting the true nature of earthquakes), it does point to a logical inconsistency in the overall model; the final distribution of segment recurrence intervals is inconsistent with that presumed in computing segment probabilities in the first place (and with how paleoseismic data are interpreted). This results from the application of a point-process model to what is ultimately not a point process.

Fortunately, in spite of the prevalence of short-recurrence-intervals, the model is pretty well moment balanced overall (the simulations have a moment rate ~3% greater than the original). Therefore, one might be willing to forgive the logical inconsistency of this model because it honors the intent of elastic rebound theory without dramatically skewing the long-term rate model. However, the problem that the implied segment recurrence-interval distribution is inconsistent with that assumed worsens as more fault segments are included in the model, and especially as we relax segmentation all together by going to a great number of very small segments. Therefore, the potential implications should be explored on a case-by-case basis (as will be done later in the context of the new S. San Andreas model that has 10 segments).

Figure 1. Example of a long-term, moment balanced rupture model for the Hayward/Rodgers-Creek fault, obtained from the WGCEP-2002 Fortran code. The image, taken from the WGCEP-2002 report, shows the segments on the left and the possible earthquakes on the right. The tables below give information including the rate of each earthquake and the rate that each segment ruptures. Note that this example represents a single iteration from their code, where modal values in the input file were given exclusive weight, aseismicity parameters were set to 1.0, no GR-tail seismicity was included, sigma of the characteristic magnitude-frequency distribution was set to zero, and the floating ruptures were given zero weight (specifically, the line on the input-file that specified the segmentation model that was given exclusive weight read: "0.11 0.56 0.26 0.07 0.00 0.00 0.00 0.00 0.00 0.00 model-A-modified")

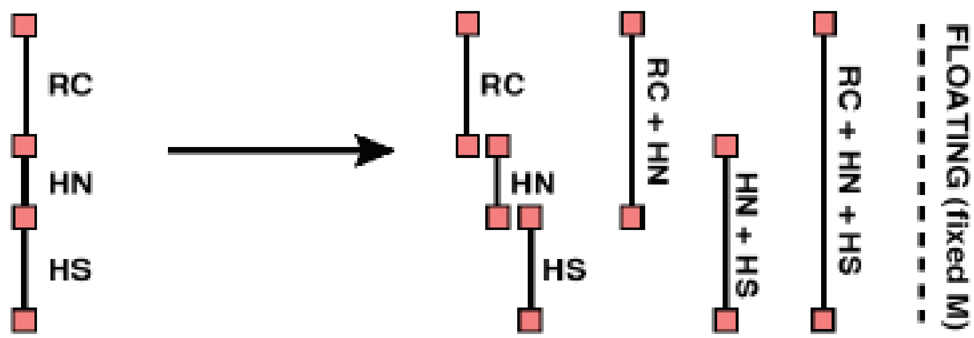

Segment Info

Name	Length (km)	Width (km)	slip-rate (mm/yr)	Rupture Rate (/yr)	Date of Last Event
HS	52.54	12	9	3.87e-3	1868
HN	34.89	12	9	3.95e-3	1702
RC	62.55	12	9	4.08e-3	1740

Earthquake Info

Name	mag	rate
HS	7.00	1.28e-3
HN	6.82	1.02e-3
HS+HN	7.22	2.16e-3
RC	7.07	3.32e-3
HN+RC	7.27	0.32e-3
HS+HN+RC	7.46	0.44e-3
floating	6.9	0

Figure 2. The BPT distribution of recurrence intervals used to compute segment rupture probabilities (red line), as well as the distribution of segment recurrence intervals obtained by simulating ruptures according the WGCEP-2002 methodology (gray bins). The BPT probabilities assume a coefficient of variation of 0.5 and the segment rates given in Figure 1. Note the relatively high rate of short recurrence intervals in the simulations.

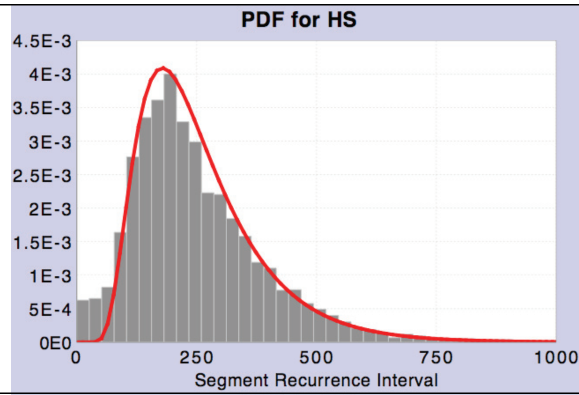

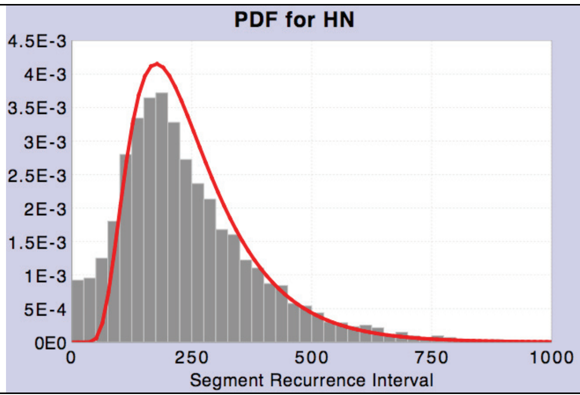

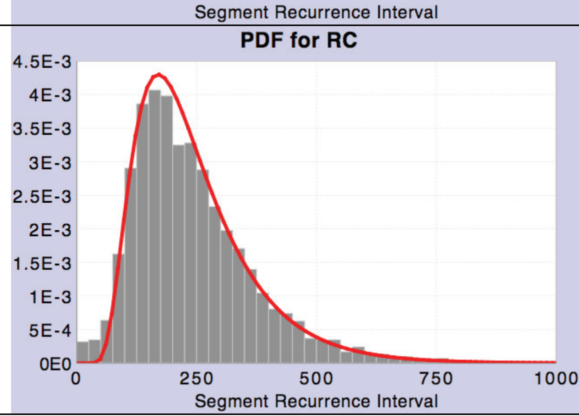

T-D Model 1:

The approach used to compute single- and multi-segment rupture probabilities in T-D Model 1 (and T-D Model 3) for the S. SAF in UCERF 1 can be stated as follows:

$$R_{td}(rup) = R(rup)\frac{\sum_{segs\_in\_rup} P'(seg)\frac{R'_{td}(seg)}{R'(seg)}}{\sum_{segs\_in\_rup} P'(seg)} \qquad (3)$$

where $R_{td}()$ is the equivalent Poisson time-dependent rate (e.g., $R_{td}(rup)$ =-ln(1-P(rup)), and as before, R() is the long-term rate and P() is the time-dependent probability (see the UCERF 1.0 documentation for the justification of this model). The primes here represent a very important distinction; namely, *the segment rates and probabilities are based on a moment-balance model that includes only single-segment ruptures*. Using the Hayward-Rodgers Creek fault in Figure 1 to exemplify, the average recurrence interval on the S. Hayward segment is 1/ 0.00387 = 258 years if both single and multi-segment ruptures are included. However, the average (moment balanced) recurrence interval is 208 years if only single segment ruptures are included. Again, the primes in the above equation indicate rates and probabilities that are based such single-segment ruptures.

For low rates of occurrence, the Poisson probability is equal to the long-term rate, so we can rewrite the above equation as:

$$P(rup) \approx P_{pois}(rup) \frac{\sum_{segs\_in\_rup} P'(seg) \frac{P'(seg)}{P'_{pois}(seg)}}{\sum_{segs\_in\_rup} P'(seg)} \quad (4)$$

If we again consider $P'(seg)/P'_{pois}(seg)$ to represent the probability gain of a segment (but this time computed assuming single-segment ruptures), the time-dependent earthquake probability computed using the above equation are essentially the time-independent earthquake probability multiplied by a weigh-averaged probability gain taken over all segments involved. Note that the weights here are based on the segment probabilities rather than segment moment rates as in the WGCEP (2003) approach above (again, see the UCERF 1.0 documentation for the justification).

To compare the implications of this model to those of the WGCEP (2003) approach, Monte Carlo simulations were again run as before, but using equation (3) to compute the earthquake probabilities. The results are qualitatively similar to those observed in Figure 2, but with the curves and bins shifted to the left since the recurrence intervals assuming single-segment ruptures are less. However, the most important manifestation of this model is that the simulated moment rate is 25% greater than that of the long-term model. In other words, there is a bias causing events to occur more often than they should. This results from two factors. Basing segment recurrence intervals on single-segment ruptures leads to lower intervals than if they are base on the entire long-term model (which includes both single and multi-segment ruptures). Lower recurrence intervals means the segment gains will exceed unity earlier in their cycle, leading to a higher probability of an event than would otherwise be the case. To confirm this, Monte Carlo simulations were run using equation (3), but where segment probabilities (or rates) were based on the average recurrence intervals considering all ruptures (un-primed values, as in the WGCEP (2003) approach). The result is qualitatively similar to that shown in Figure 2, but with a remaining positive moment-rate bias of 14%.

The other source of bias results from using the segment probabilities as weights in computing the average probability gain. This also skews the probabilities toward higher values, leading to an increased effective moment rate. Changing the weights in equation (3) to segment areas, and using un-primed segment probabilities, leads to results that are indistinguishable from the WGCEP (2003) result in Figure 2 (including the positive moment-rate bias of ~3%). It's worth noting that these Monte Carlo simulations were based on the BPT distribution, whereas the S. SAF probabilities given in the UCERF 1.0 report were computed using a log-normal distribution; this difference does not influence the problem just discussed.

Given the 25% moment-rate bias found in using equation (3) in the Hayward-Rodgers Creek simulations, the obvious question is what this implies for the T-D Model 1 (and T-D Model 3) UCERF 1.0 probabilities on the S. SAF (where it was actually applied). Based on the above result, one might expect the probabilities to be too high. However, this is generally not the case as outline next.

Table 1 lists the 30-year conditional probabilities for S. SAF in UCERF 1.0 for T-D Model 1 (computed using equation (3) above using a log-normal distribution for each segment). Also listed are probabilities computed using equation (3), but where the segment probabilities are not based on only single-segment ruptures (that is, the alternative, un-primed values were used). Opposite to what is suggested by the above simulations, all but one of the earthquake probabilities are lower using equation (3) than with the alternative, un-primed values. The biggest difference is for a single-segment rupture of the Cholame segment (a 35% difference).

To understand why this is the case, consider the data used to compute their segment probabilities listed in Table 2 here. Specifically, consider the Coachella Valley segment. The median recurrence interval for this segment considering only single-segment ruptures is 71 years, whereas that considering both single and multi-segment ruptures is 154 years (T_{med} and Alt. T_{med} in Table 2, respectively). At first glance one would expect the gain to be higher in the former because the shorter recurrence interval means the gain exceeds unity at an earlier date. However, this is not the case as can be seen in Table 2. The reason is that it has been 316 years since the last event. With T_{med} =71 years, we are 316/71= 4.4 times the median recurrence interval into the current cycle (for which, incidentally, there is only a ~1% probability of making it past this point). For T_{med} Alt. = 154, we are 316/154 = 2.0 times the median recurrence interval into the current cycle. Because the hazard rate function of the lognormal-distribution begins to decline just past the median interval, 30-year probabilities for the Coachella Valley are presently declining with time (the gains are going down), and they have gone down even more for the 71-year median interval than for the 154-year interval (see Figure 3 for an illustration). Because T-D Model 3 of UCERF 1.0 also uses equation (3) with the exact same segment gains, it too has some significantly different probabilities. Because the results are sensitive to the behavior of the hazard-rate function out on the tails, different probabilities would be obtained using a BPT model.

Table 1. The S. SAF earthquake probabilities obtained using Model 1 of UCERF 1.0 ("Orig. Prob."), as well as alternative probabilities ("Alt. Prob.") obtained using segment recurrence intervals considering both singe and multi-segment ruptures. The ratio of the two is listed as "Alt./Orig.". Note that these probabilities include an 11% Poisson contribution (as stipulated for the final UCERF 1.0 probabilities), so the pure time-dependent differences are slightly greater.

Earthquake	Orig. Prob.	Alt. Prob.	Alt./Orig.
Coachella only	0.00129	0.00168	1.30
San Bernardino only	0.00140	0.00134	0.96
Mojave only	0.00138	0.00171	1.23
Carrizo only	0.00185	0.00186	1.00
Cholame only	0.00237	0.00319	1.35
Cholame to Coachella	0.00190	0.00217	1.14
1857 Rupture	0.00412	0.00482	1.17
San Bern. & Coachella	0.00406	0.00439	1.08

Table 2. Data used to compute probabilities on the S. SAF segments. T_{med}, Prob, and Gain are the median recurrence interval, the 30-year probability (based on a log-normal distribution), and the Gain relative to a Poisson model, respectively, assuming single-segment ruptures only (corresponding to the primed values in Equation (3)). The "Alt." values are those obtained using segment recurrence intervals considering both single and multi-segment ruptures (un-primed values).

T_{last}	T_{last}	2006- T_{last}	σ	T_{med}	Prob	Gain	Alt. T_{med}	Alt. Prob	Alt. Gain
Coachella	1690	316	0.63	71	0.325	1.14	154	0.215	1.52
San Bern.	1812	194	0.53	112	0.358	1.92	176	0.238	1.84
Mojave	1857	149	0.80	56	0.342	1.06	122	0.215	1.34
Carrizo	1857	149	0.58	74	0.442	1.69	145	0.256	1.69
Cholame	1857	149	0.66	37	0.512	1.11	118	0.271	1.54

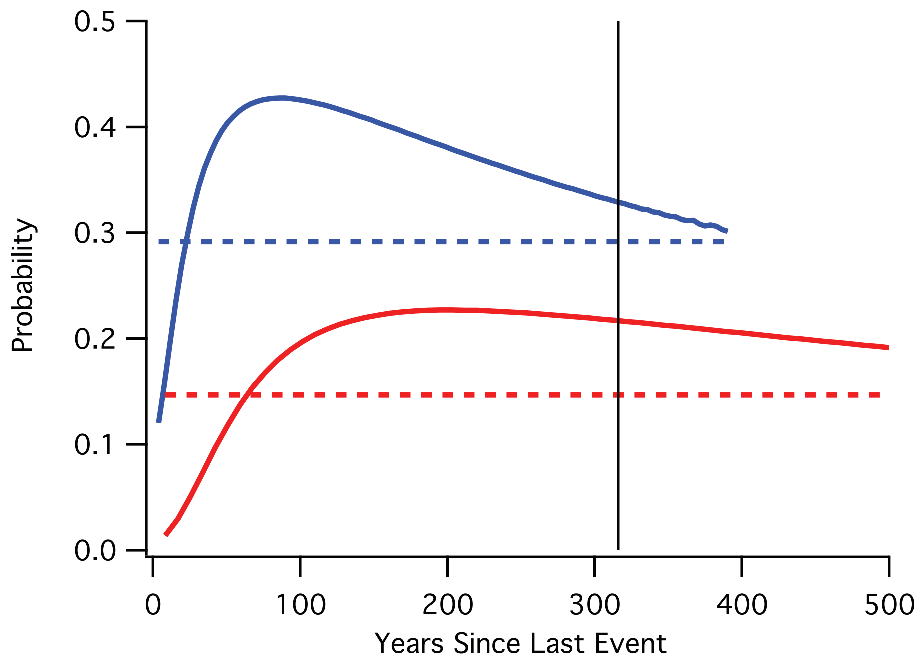

Figure 3. The 30-year probability for a Coachella-Valley-segment rupture as a function of time since the last event (i.e., the 30-year hazard rate). Blue curves are for a median recurrence interval of 71 years, and red lines are for a median of 154. The solid lines are for a log-normal distribution, and the dotted lines are for a Poisson distribution. The probability gain is therefore the ratio of the solid to dotted lines. The vertical black line at 316 years marks the implied 30-year probabilities in 2006, the beginning of the UCERF 1.0 forecast, given the date of last event was 1690. Note that at this time the 30-year time-dependent probabilities are decreasing, and are closer to the Poisson values for the 71-year median recurrence interval (which therefore has a lower probability gain).

T-D Model 2:

In terms of repeated application of this methodology as earthquakes occur, there is a fundamental problem that negative (i.e., non-physical) rates can arise. For example, if the Cholame segment ruptured alone today (which it can according to the long-term model), the rate of such events would subsequently become negative (confirmed by setting the date of last rupture for this segment to 2005 in the Excel spreadsheet used for their calculations). We therefore no longer consider this a viable model, and therefore do not discuss it further.

Conditional Time-Dependent Probabilities for UCERF 2

As with UCERF 1 and the WGCEP (2003) model, UCERF 2 applies probabilities to a long-term rate model from each branch of the logic-tree. By definition, Type-A faults in UCERF 2 have sufficient information to compute conditional probabilities based on dates of previous events. Of the previously published methods outlined above for computing conditional probabilities when both single- and multi-segment ruptures are included (which are needed because none of our Type-A faults invoke strict segmentation), that of WGCEP (2003) appears to be best-available science. However, as exemplified above, this methodology has a logical inconsistency in that the segment recurrence intervals implied by the model are inconsistent with those assumed in the first place. This issue appears to be relatively minor when faults are represented with only a few segments, as was the case in WGCEP (2003) where only up to four segments were used for any given fault. UCERF 2, on the other hand, utilizes more segments for three faults in southern California, with the maximum being 10 segments for the S. SAF. The onus is therefore upon us to demonstrate that the WGCEP (2003) approach is adequate in this case. Before presenting such simulations tests, additional discussion of logic tree branches is in order.

Logic-Tree Branches

The long-term rate model includes both a segmented and un-segmented branch for Type-A faults (Figure 4 in main report). Of these two, only the segmented branch has the option for time-dependent conditional probabilities because of current difficulties in applying such a model where segmentation is relaxed. Excluding the un-segmented option, there are a total of 12 different long-term-rate models (final branches) for which conditional, time-dependent probabilities can be computed for each fault. These branches are shown in Figure 4 (see the main report and/or Appendix G for further discussion of these branches and consequent models). From each of these, two alternative branches exist for computing conditional probabilities: one assuming a constant aperiodicity for all segments, where three alternative values are specified on subsequent branches, and one where the segment-specific aperiodicities listed in Table 4 are used (derived from paleosiesmic data as described in Appendix C, and listed in Table 9 therein) where the default value is 0.5 if no segment-specific value is available. This latter branch is also depicted in Figure 4. The justification for these aperiodicity choices is given in the main part of this report. Given the full logic tree, there are up to 48 different conditional time-dependent probability models for each Type-A fault.

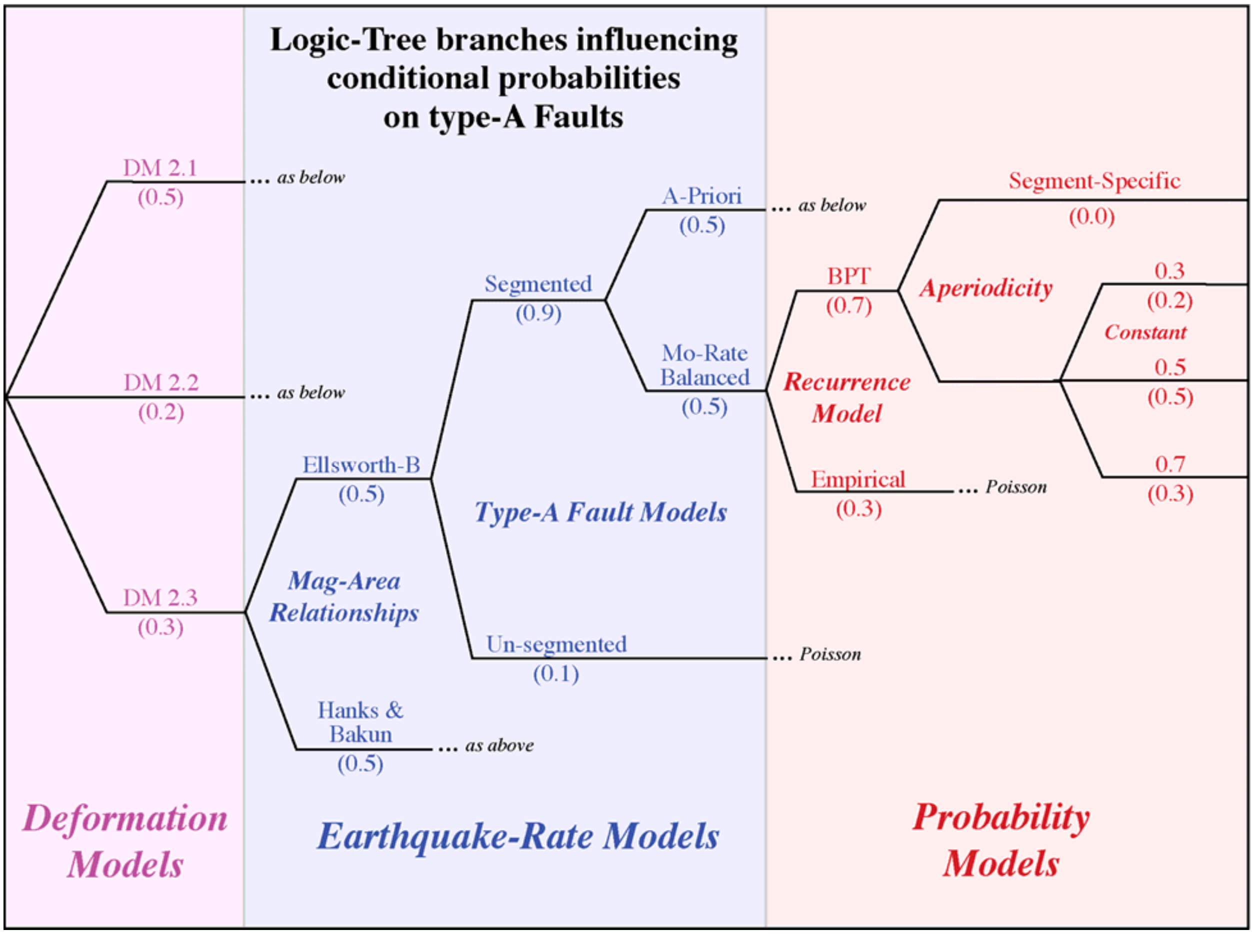

Figure 4. Logic-tree branches influencing the conditional, time-dependent probability calculations on Type-A faults. There are 12 different long-term rate model branches leading into the segmented BPT-model, and up to four additional branches in getting from there to the final probabilities (although the segment-specific aperiodicity branch is given zero weight for reasons discussed in the text).

Simulation Results for the S. SAF

Returning to the discrepancy between assumed and implied segment recurrence intervals in the WGCEP (2003) BPT Model, there are two questions of interest here: 1) how much worse is this discrepancy for the 10-segment S. SAF model (as opposed to the 3-segment example given above in Figure 2); and 2) are segment-specific aperiodicities really warranted given this distortion of the assumed probability distribution? Simulation results for the S. SAF (computed just as describe for the Hayward-Rodgers Creek case above) are shown in Figure 5. Only one branch of the long-term rate model was used in for this simulation (*Deformation Model = DM 2.1*, *Mag-Area Relationship= Ellsworth B*; and moment-balanced model). The constant aperiodicity of 0.5 versus segment-specific aperiodicity results are shown to the left and right side of the figure, respectively. The discrepancy between the assumed and simulated segment recurrence interval is indeed worse than in the three-segment case of Figure 2. Fortunately, the overall shape is generally preserved and there is no significant bias in the rate of each rupture or in the overall moment rate (all within about 3%). However, the working group decided that it would be inappropriate to apply segment-specific aperiodicities given the difference between the assumed and simulated distributions (thus the zero branch weight given in Figure 4); results for this case are nevertheless given below for interested readers.

Figure 5. Segment recurrence intervals assumed (red) and simulated (gray bins) for the southern San Andreas Fault. The right side shows results assuming a constant aperiodicity of 0.5 among segments and the right side show results for segment-specific values (as labeled) from Appendix C. The simulations were conducted exactly as described for the Hayward-Rodgers Creek example described in the text. The relationships between segment abbreviations and the names of the associated fault sections are as follows: PK=Parkfield; CH=Cholame, rev; CC=Carrizo, rev; BB=Big Bend; NM=Mojave N; SM=Mojave S; NSB=San Bernardino N; SSB=San Bernardino S; BG=San Gorgonio Pass-Garnet Hill; CO=Coachella, rev.

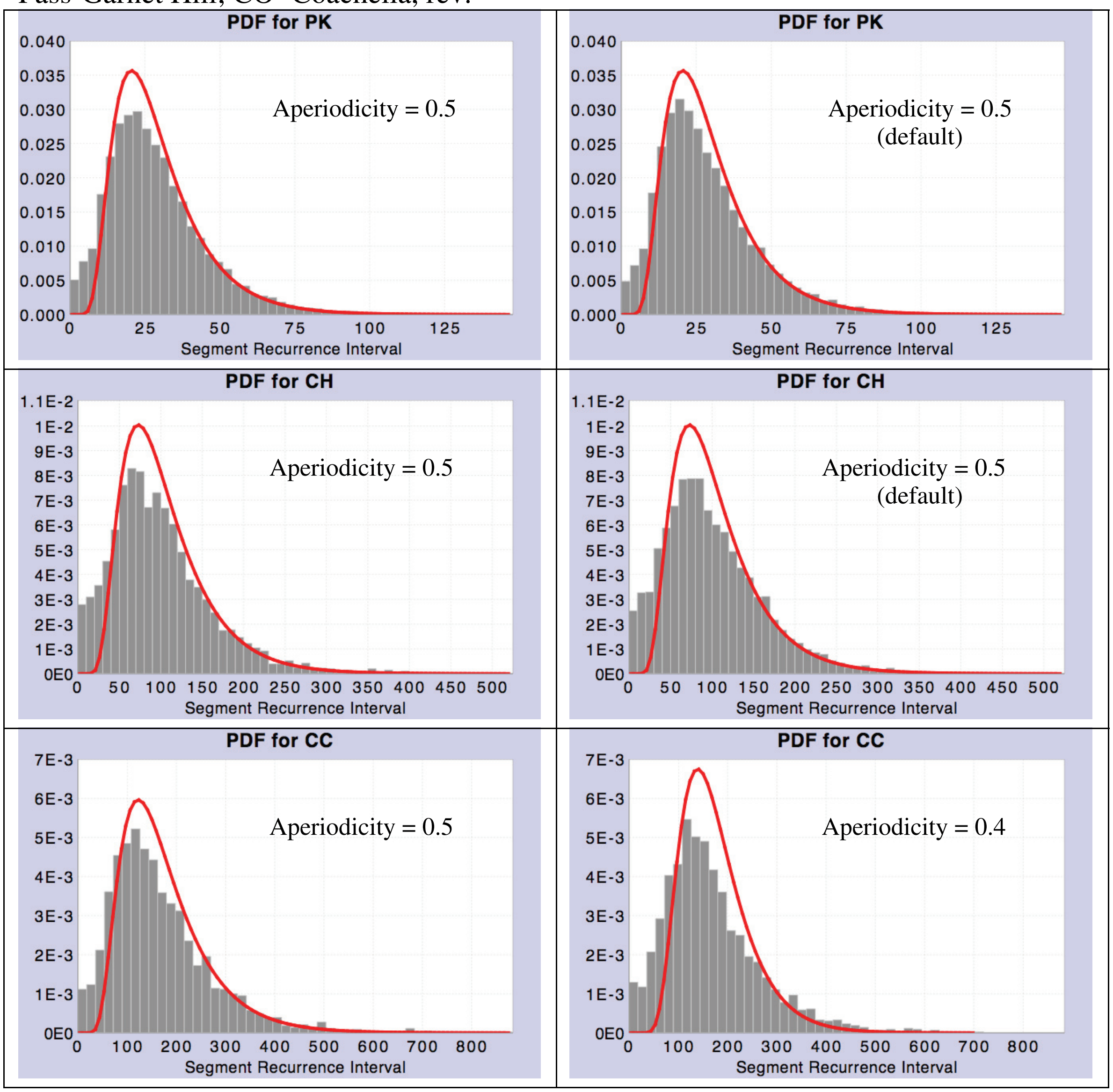

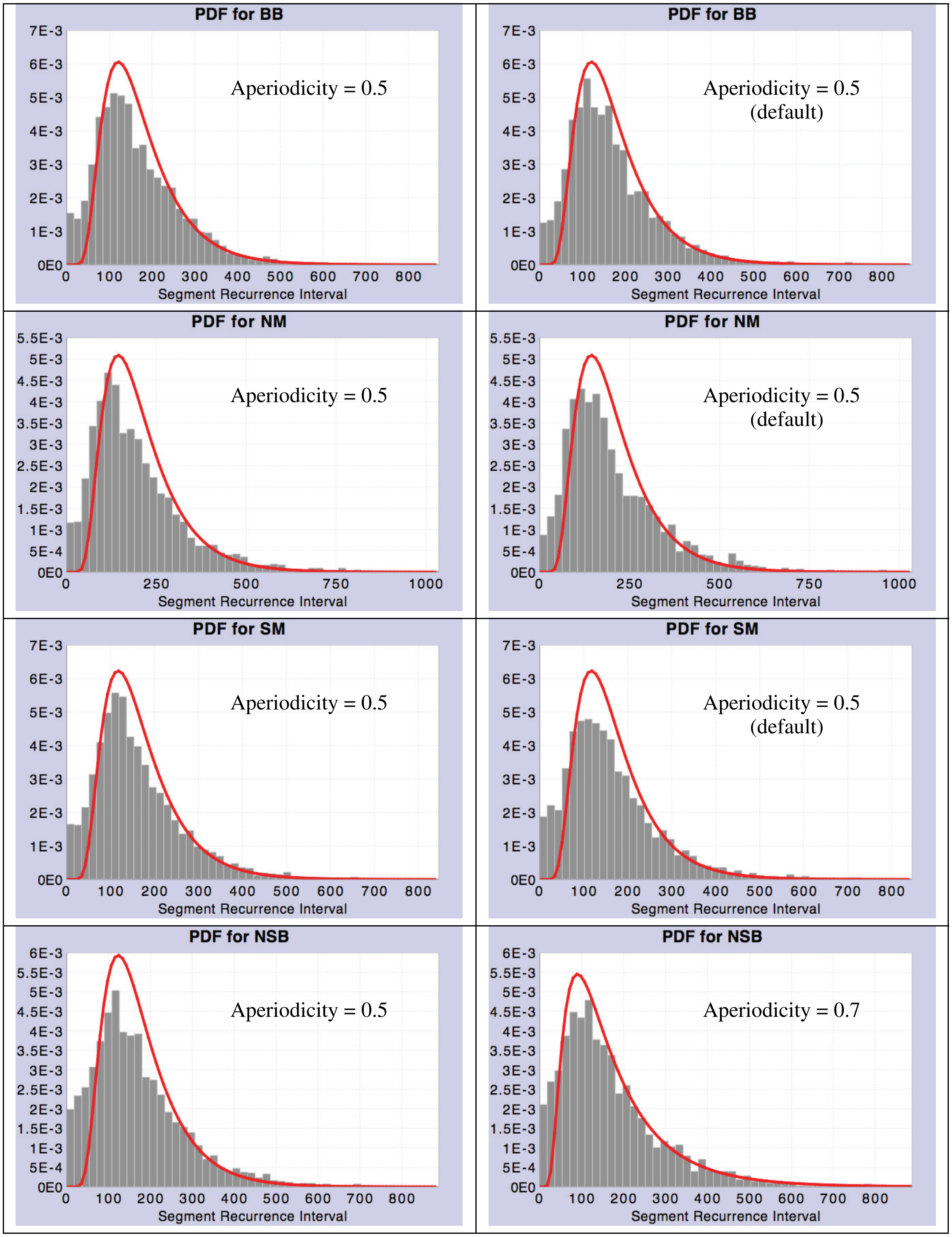
PDF for BB
Aperiodicity = 0.5
Segment Recurrence Interval
PDF for BB
Aperiodicity = 0.5
(default)
Segment Recurrence Interval
PDF for NM
Aperiodicity = 0.5
Segment Recurrence Interval
PDF for NM
Aperiodicity = 0.5
(default)
Segment Recurrence Interval
PDF for SM
Aperiodicity = 0.5
Segment Recurrence Interval
PDF for SM
Aperiodicity = 0.5
(default)
Segment Recurrence Interval
PDF for NSB
Aperiodicity = 0.5
Segment Recurrence Interval
PDF for NSB
Aperiodicity = 0.7
Segment Recurrence Interval

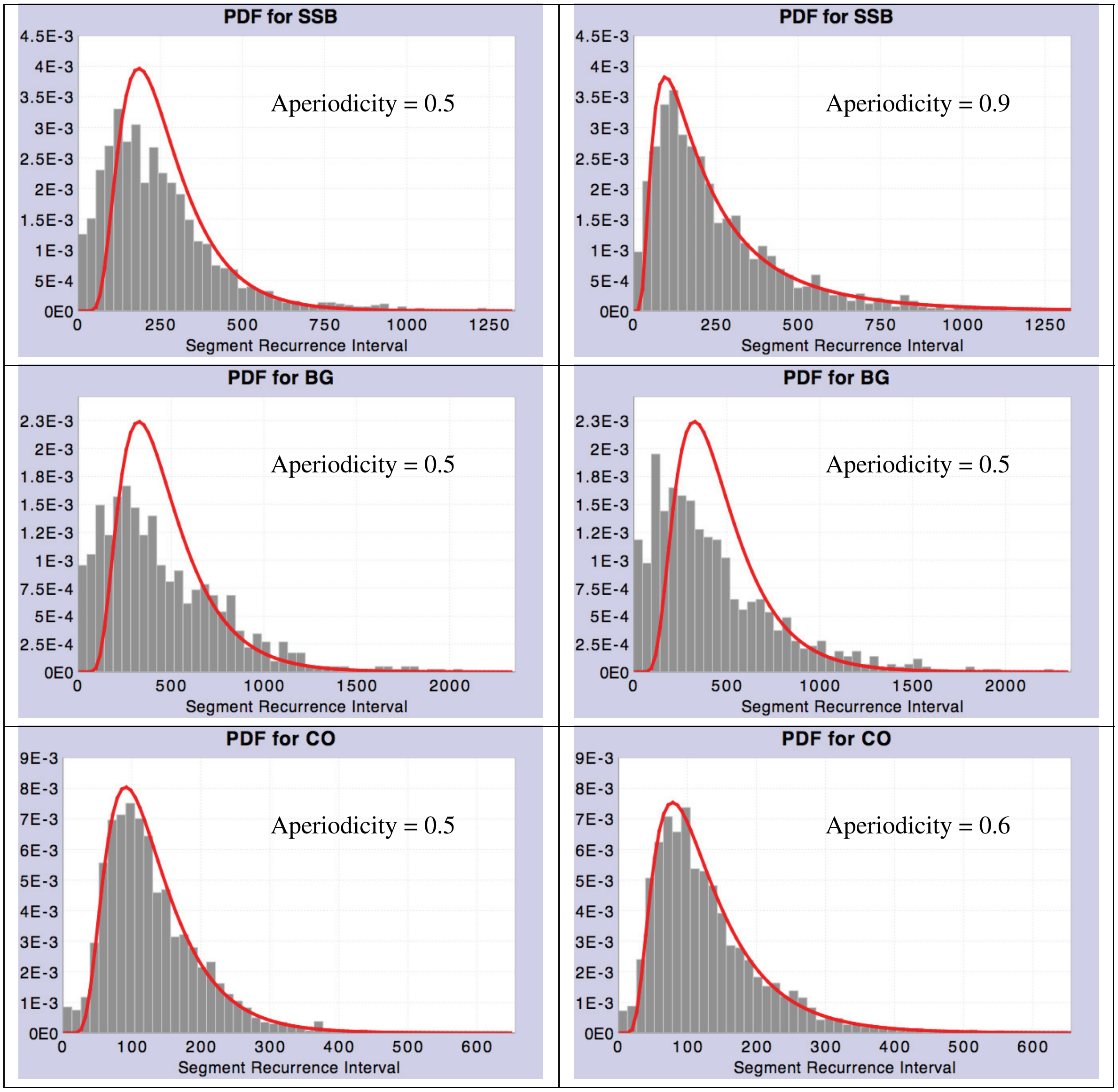
PDF for SSB
Aperiodicity = 0.5
4.5E-3 4E-3 3.5E-3 3E-3 2.5E-3 2E-3 1.5E-3 1E-3 5E-4 0E0
0 250 500 750 1000 1250
Segment Recurrence Interval
PDF for SSB
Aperiodicity = 0.9
4.5E-3 4E-3 3.5E-3 3E-3 2.5E-3 2E-3 1.5E-3 1E-3 5E-4 0E0
0 250 500 750 1000 1250
Segment Recurrence Interval
PDF for BG
Aperiodicity = 0.5
2.3E-3 2E-3 1.8E-3 1.5E-3 1.2E-3 1E-3 7.5E-4 5E-4 2.5E-4 0E0
0 500 1000 1500 2000
Segment Recurrence Interval
PDF for BG
Aperiodicity = 0.5
2.3E-3 2E-3 1.8E-3 1.5E-3 1.2E-3 1E-3 7.5E-4 5E-4 2.5E-4 0E0
0 500 1000 1500 2000
Segment Recurrence Interval
PDF for CO
Aperiodicity = 0.5
9E-3 8E-3 7E-3 6E-3 5E-3 4E-3 3E-3 2E-3 1E-3 0E0
0 100 200 300 400 500 600
Segment Recurrence Interval
PDF for CO
Aperiodicity = 0.6
9E-3 8E-3 7E-3 6E-3 5E-3 4E-3 3E-3 2E-3 1E-3 0E0
0 100 200 300 400 500 600
Segment Recurrence Interval

Earthquake Rupture Probabilities for All Logic Tree Branches

The date of previous event (from Appendix B), average mean recurrence interval, and segment-specific aperiodicity (from Appendix C where available) are listed in Table 4. The segment and earthquake-rupture probabilities obtained using the WGCEP (2003) approach (Equation (1)) are listed for all 36 non-zero-weighted logic-tree branches (Figure 4), and for all faults, in the following Excel files (a different file for a forecast duration of 5 vs 30 years, where each has a start-year of 2007):

RupProbs_BPT_5yr_ConstAperBranches.xls

RupProbs_BPT_30yr_ConstAperBranches.xls

(available from: http://gravity.usc.edu/WGCEP/resources/documents/UCERF2_FinalReport)

The above files also contain gains (time-dependent probabilities divided by Poisson probabilities), aggregated earthquake probabilities for each fault, and minimum, maximum, and average values over all logic tree branches (see the "README" tab for a full explanation). Tables 5 and 6 here (at the end of this document) summarize the 5-year segment and rupture probabilities, respectively. Those interested in results from the 12 logic-tree branches where the segment-specific aperiodicities are applied (given zero weight in our final model as discussed above) can find them at:

RupProbs_BPT_5yr_SegDepAper.xls

RupProbs_BPT_30yr_SegDepAper.xls

(available from: http://gravity.usc.edu/WGCEP/resources/documents/UCERF2_FinalReport)

Discussion

As discussed above, we believe the WGCEP (2003) methodology for computing conditional time-dependent probabilities for single- and multi-segment ruptures represents best available science in terms of published approaches. However, issues exist with respect to a difference between assumed and implied segment recurrence-interval probability distributions, and this discrepancy gets worse as the number of segments increases. For example, Figure 6 shows simulation results for a more extreme case of an 80-km fault divided into 16 segments of 5-km-length each (essentially un-segmented), where the magnitude-frequency distribution of the fault was specified as Gutenberg-Richter with a b-value of 1.0 (the a-value is not important for the point being made here). As described above, events were simulated using the WGCEP (2003) methodology (Equation (1)) assuming an aperiodicity of 0.25 on each segment, and segment recurrence intervals were tallied. Figure 6, which shows the behavior averaged over all segments, reveals a major discrepancy between the assumed and simulated segment recurrence-intervals. Furthermore, the rates of events and total moment rate from the simulation is about 20% high (a significant discrepancy). Unfortunately this problem cannot be fixed by adjusting the assumed segment recurrence-interval distributions ("stacking the deck" so to speak), as there will always be a difference between the before and after distribution (implying an inherent conceptual problem). This problem ultimately results from the fact that we are attempting to apply a point-process model to a non-point process (we are not accounting for the correlation of earthquake probabilities caused by interactions).

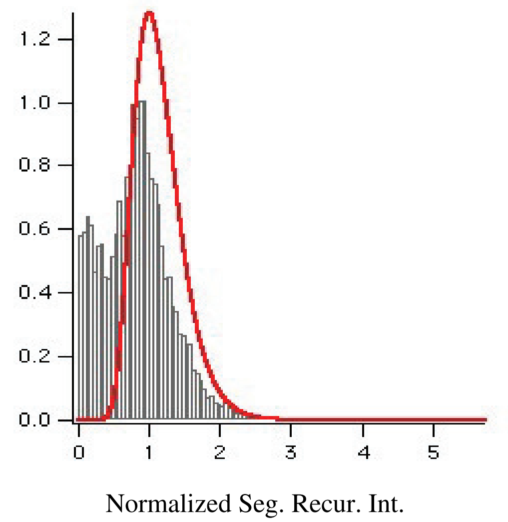

Figure 6. Probability distribution of segment recurrence intervals assumed (red) and from Monte-Carlo simulations (gray bins) for an 80 km fault with 5-km segments (essentially un-segmented) with a Gutenberg-Richter distribution of events and using the WGCEP (2003) methodology for computing time-dependent probabilities (see text for details).

Possible Alternative Approaches

Given a general desire within the current working group to relax segmentation assumptions, except where demanded by data, considerable effort has been put into searching for alternative, internally consistent approaches for computing elastic-rebound-motivated probabilities under these conditions. Only a brief, verbal description of this quest is given here since we have not yet found an alternative that we are ready to advocate the use of. The discussion here has benefited greatly from exploring synthetic catalogs generated from two physics-based earthquake simulators, "Virtual California" of Rundle et al. (2004) and the simulator of Ward (2000), both of which exhibit elastic-rebound behavior while not imposing any segmentation.

In the absence of additional information (such as date of last event) we generally revert to Poisson probabilities based on the average rate of each event (written $P_{pois}(Rup_i)$, where index i refers to the i^{th} rupture). Therefore, one approach is to devise a rational scheme for modifying these time-independent probabilities when other data are available. Bayes' theorem provides one particularly intriguing possibility, which in our context can be written as:

$$P(Rup_i \mid D) = \frac{P_{pois}(Rup_i)P(D \mid Rup_i)}{\sum_i P_{pois}(Rup_i)P(D \mid Rup_i)}$$

This says that the relative probability of a particular rupture (Rup_i), given other "data" D, is simply the Poisson probability of that rupture (the prior distribution) scaled by the probability that the additional data (D) is consistent with the occurrence of that rupture (and not that the data are actually *caused* by that rupture). The $P(D|Rup_i)$ term is referred to as the likelihood function in Bayes' theorem, and can be though of here as a probability gain for that rupture. Two obvious candidate likelihood functions for elastic-rebound-motivated probabilities are as follows:

1) *Average Slip Predictable Model* – this would quantify whether enough time has passed since the last event(s) along the fault to accommodate the slip needed for that that rupture (Rup_i). The expected date of each rupture could be set as exactly when the associated amount of slip had accumulated, with aleatory uncertainty in the actual date being represented with a BPT distribution (or some other reasonable model). Note that no assumptions of segmentation or characteristic earthquakes are required here, as the previous event(s) could have occurred anywhere along the fault. The BPT model is used only to represent the probability distribution for the possible occurrence times of a given hypothesized event (assuming it will be the next to occur), and does not represent an actual recurrence of anything. In fact, a given rupture need never recur to the extent there are an infinite number of starting and ending points along the fault. The name assigned to this likelihood function comes from the fact that it's a generalization (or more specifically an along-fault averaging) of the Slip-Predictable model introduced by Shimazaki and Nakata (1980).

2) *Average Time Predictable Model* – this likelihood function is exactly like the *Average Slip Predictable Model* above, except the expected time of rupture at each point on the fault is when the amount of slip in the *previous* earthquake at that point has accrued. Again, the name has been assigned according to the fact that it represents a spatial averaging of the Slip Predictable model introduced by Shimazaki and Nakata (1980).

One problem with the Bayesian approach outlined above is that it only gives the relative probability of various ruptures (and not absolute probabilities). Therefore, it would only be useful in a situation where the total probability, when aggregated over all ruptures, remains constant (or at least any variability is quantifiable using information other than the data (D) used in Bayes' theorem). In other words, if any ruptures are deemed relatively likely, then there must be another set that are relatively unlikely (such that the total probability or rate has not changed). Therefore, this approach is not applicable to individual faults (in isolation) if one desires to interpret, for example, a full-fault rupture as implying the probabilities of all ruptures on that fault have declined. Nevertheless, Monte Carlo simulations conducted by applying the above Bayes' theorem approach to a system of faults with the average time-predictable likelihood function appear promising (no significant biases or conceptual inconsistencies). Therefore, this approach might be useful if and when we can apply the methodology to a broad-enough range of faults (again, such that the total probability of an event remains relatively constant). The average slip-predictable model does not work, however, because smaller events require less slip and are therefore preferentially chosen (due to their relatively high probability gains) earlier in the cycle.

The Bayesian approach just outlined inspired us to search for other possible approaches that might give absolute probabilities in the situation where segmentation assumptions are relaxed (and not requiring the application to an entire fault system). Let's hypothesize that a given rupture will be the one to occur next, so all we are left to do is define when it will occur. We can define an expected Average Time-Predictable time interval as

$$\Delta t_{\exp}^{time-pred} = t_{\exp}^{time-pred} - t_{last}^{time-pred}$$

where $t_{\exp}^{time-pred}$ is the average expected time at which the slip in the last event has recovered, and $t_{last}^{time-pred}$ is the average date of last event (more detailed equations are available upon request). The ratio of the actual time interval (an aleatory uncertaianty) to this expected time interval can be represented with a BPT distribution (or any other reasonable renewal model) with mean of 1.0. The probability of the event occurring in any given time interval, which we write $P_{BPT}^{slip-pred}(rup)$, can be computed in the customary fashion. The problem now is that this event might not be the next to occur, and we can't simply aggregate the probabilities all possible ruptures in the usual way (assuming independence) because any spatial overlap of ruptures means the probabilities are correlated. It turns out that the following equation works well:

$$P(rup) = P_{Pois}(rup)\frac{P_{BPT}^{slip-pred}(rup)}{P_{Pois}^{slip-pred}(rup)}$$

where $P_{Pois}(rup)$ the Poisson probability of a given rupture (based on the rate of each rupture in the long-term model) and $P_{Pois}^{slip-pred}(rup)$ is the Poisson probability based on $\Delta t_{\exp}^{time-pred}$. In saying that this works well, we mean that Monte Carlo simulations exhibit the desired effect (elastic-rebound type behavior in an un-segmented model) without biasing rates in the long-term model. An equivalent formulation for an Average Slip-Predictable model, where the expected time is when the slip for the forthcoming event has accumulated, does not work because smaller events have relatively higher gains early on, and are therefore preferentially chosen in the simulation (significantly biasing the rates and magnitude-frequency distribution of the long term model).

In spite of the promising results with respect to the above Average Time-Predictable model, the following two issues need to be considered more carefully before application is warranted: 1) the method requires having slip-in-previous-event data which are generally sparse and/or highly uncertain (so it's not clear what the net benefit would be after propagating all relevant uncertainties); 2) the aperiodicity at a point on the fault is generally much higher than that used in computing $P_{BPT}^{slip-pred}(rup)$, so considerable hand "tuning" would be required to match observed aperiodicities at locations like those compiled in Appendix C.

Finally, note that none of the procedures discussed here represent physics-based approaches. Rather, they are physically motivated statistical rules aimed at modifying long-term rates (or Poisson probabilities) so as to be closer to what we expect on the basis of elastic-rebound theory. This is consistent with the Bayesian notion that probability is a subjective statement of "the degree of belief that an event will occur" (D'Agostini, 2003, http://www-zeus.roma1.infn.it/~agostini/rpp/). That being said, perhaps the overall approach of modifying long-term rates (or Poisson probabilities) based on simple rules is misguided. For example, just because the slip-predictable approaches discussed above lead to a biased result, compared to the long-term model, this does not mean there is nothing to the notion that an event occurring sooner will more likely be smaller. Perhaps physics-based simulators, which make no distinction between a long-term-rate model and time dependent behavior, will be a more fruitful line of enquiry.

Conclusions

In spite of some conceptual issues, the WGCEP (2003) methodology for computing probabilities when both single- and multi-segment ruptures are included remains the best available science, and is therefore the approach adopted here. In particular, it honors the intent of elastic-rebound motivated recurrence models in terms of lowering probabilities immediately after an event. Segment-specific aperiodicities, however, are not warranted given the recurrence-interval distortion discussed above, as well as the mild influence on the results. The final, weight-average probabilities for the time-dependent type-A fault segmented models are given as the "BPT Wt Ave" values listed in Table 6. A fault-by-fault comparison of earthquake rupture probabilities with those of previous studies is given in the main body of this report.

References

Field, E.H. (2007). A Summary of Previous Working Groups on California Earthquake Probabilities, *Bull. Seism. Soc. Am. In Press*.

Matthews, M.V., W.L. Ellsworth, and P.A. Reasenberg (2002). A Brownian Model for Recurrent Earthquakes, *Bull. Seism. Soc. Am.* **92**, 2233–2250.

Petersen, M.D., T. Cao, K.W. Campbell, and A.D. Frankel (2007). Time-independent and Time-dependent Seismic Hazard Assessment for the State of California: Uniform California Earthquake Rupture Forecast Model 1.0, *Seism. Res. Lett.* **78**, 99-109.

Rundle, J.B., P.B. Rundle, A. Donnellan, and G. Fox (2004). Gutenberg-Richter statistics in topologically realistic system-level earthquake stress-evolution simulations, •*Earth Planets Space* **56**, 761-771.

Shimazaki, K., and Nakata, T. (1980). Time-predictable recurrence model for large earthquakes, *Geophys. Res. Lett.* **7**, 279-282.

Ward, S.N. (2000). San Francisco Bay Area Earthquake Simulations: A Step Toward a Standard Physical Earthquake Model, *Bull. of the Seism. Soc. Am.* **90**, 370–386.

Working Group on California Earthquake Probabilities (1988). Probabilities of large earthquakes occurring in California on the San Andreas fault, *U.S. Geological Survey Open-File Report*, p. 62.

Working Group on California Earthquake Probabilities (1990). Probabilities of large earthquakes in the San Francisco Bay Region, California, *U.S. Geological Survey Circular*, p. 51.

Working Group on California Earthquake Probabilities (2003). Earthquake Probabilities in the San Francisco Bay Region: 2002–2031, *USGS Open-File Report* **03-214**.

Table 4. Segment data, including best-estimates of date of last event (from Appendix B) and Aperiodicity (from Appendix C). "Wt Ave Recurrence Interval" is the average recurrence interval considering the first 12 branches in Figure 4 (the ones that influence the long-term rate model) and their respective weights. "Max Recurrence Interval" and "Min Recurrence Interval" correspond to the extreme values observed among all 12 logic-tree branches. The recurrence intervals are listed only for illustrative purposes, as the branch-specific values are used in actual probability calculations.

Segment Name	Last Event (Calendar yr)	Aperiodicity	Wt Ave Recurrence Interval	Max Recurrence Interval	Min Recurrence Interval
Elsinore					
W	207	0.5	1090	604	1395
GI	1910	0.7	369	272	582
T	1732	0.7	692	500	960
J	807	0.5	1499	1000	1991
CM	1892		701	357	931
Garlock					
GE	1000		903	780	967
GC	1540	0.7	1013	733	1275
GW	1695	0.5	936	714	1158
San Jacinto					
SBV	1769		330	214	490
SJV	1918		252	206	311
A	1795		249	207	292
C	1795		353	238	582
CC	1892		420	371	467
B	1968		281	130	433
SM	1540	0.7	305	194	376
N. San Andreas					
SAO	1906		218	200	229
SAN	1906	0.6	261	246	295
SAP	1906		246	220	294
SAS	1906	0.3	193	157	213
S. San Andreas					
PK	2004		24	16	30
CH	1857		118	85	142
CC	1857	0.4	173	156	205
BB	1857		180	172	197
NM	1857		190	155	252
SM	1857		155	129	208
NSB	1812	0.7	175	145	208
SSB	1812	0.9	244	199	405
BG	1680	0.5	398	224	1002
CO	1680	0.6	156	61	214

Hayward-Rogers Creek					
RC	1758		210	163	291
HN	1715	0.6	150	109	204
HS	1868	0.6	158	112	219
Calaveras					
CN	1775	0.4	381	188	484
CC	1982		77	42	89
CS	1899		50	19	71

Table 5. For a start-year of 2007 and a forecast duration of 5-years, this list the following for each segment: "BPT Wt Ave" - average conditional time-dependent probability considering all 36 non-zero-weighted logic-tree branches; "BPT Min" – the minimum time-dependent probability among the same 36 logic-tree branches; "BPT Max" – the maximum time-dependent probability among the same 36 logic-tree branches; "Pois Wt Ave" – the average Poisson probability; "BPT Gain" – the ratio of "BPT Wt Ave" to "Pois Wt Ave".

Segment Name	BPT Wt Ave	BPT Min	BPT Max	Pois Wt Ave	BPT Gain
Elsinore					
W	1.31E-02	4.54E-03	4.81E-02	5.14E-03	2.55
GI	5.36E-03	3.27E-11	1.67E-02	1.48E-02	0.36
T	6.28E-03	3.10E-06	1.32E-02	7.81E-03	0.80
J	6.80E-03	1.42E-03	1.87E-02	3.73E-03	1.83
CM	1.51E-03	4.63E-16	1.12E-02	8.28E-03	0.18
Garlock					
GE	1.20E-02	7.61E-03	2.39E-02	5.56E-03	2.15
GC	5.36E-03	5.74E-05	9.87E-03	5.27E-03	1.02
GW	2.98E-03	7.97E-07	7.94E-03	5.63E-03	0.53
San Jacinto					
SBV	3.14E-02	2.08E-03	7.78E-02	1.74E-02	1.80
SJV	1.15E-02	1.11E-05	2.71E-02	2.04E-02	0.56
A	3.60E-02	2.47E-02	7.35E-02	2.01E-02	1.80
C	2.38E-02	1.31E-04	5.15E-02	1.59E-02	1.50
CC	3.31E-03	5.02E-07	1.06E-02	1.20E-02	0.28
B	6.66E-03	6.58E-21	2.89E-02	2.46E-02	0.27
SM	4.20E-02	2.11E-02	1.29E-01	1.73E-02	2.43
N. San Andreas					
SAO	1.87E-02	2.38E-03	3.15E-02	2.27E-02	0.82
SAN	1.15E-02	1.38E-04	2.27E-02	1.91E-02	0.60
SAP	1.42E-02	1.48E-04	2.73E-02	2.04E-02	0.70
SAS	2.73E-02	4.58E-03	4.47E-02	2.60E-02	1.05
S. San Andreas					

PK	5.04E-02	2.25E-06	2.33E-01	1.99E-01	0.25
CH	9.69E-02	5.21E-02	2.50E-01	4.33E-02	2.24
CC	5.31E-02	3.48E-02	8.86E-02	2.89E-02	1.84
BB	4.93E-02	3.65E-02	6.80E-02	2.75E-02	1.79
NM	4.69E-02	1.43E-02	8.93E-02	2.69E-02	1.74
SM	6.61E-02	3.47E-02	1.35E-01	3.27E-02	2.03
NSB	6.11E-02	3.59E-02	1.33E-01	2.83E-02	2.16
SSB	3.81E-02	2.39E-03	7.42E-02	2.12E-02	1.80
BG	3.30E-02	1.73E-05	9.68E-02	1.58E-02	2.09
CO	9.27E-02	3.37E-02	3.59E-01	3.85E-02	2.41
Hayward-Rogers Creek					
RC	5.53E-02	2.54E-02	1.32E-01	2.46E-02	2.25
HN	8.49E-02	3.54E-02	2.20E-01	3.43E-02	2.47
HS	6.33E-02	2.17E-02	1.60E-01	3.30E-02	1.92
Calaveras					
CN	2.28E-02	1.88E-03	9.67E-02	1.50E-02	1.51
CC	5.10E-02	1.02E-04	1.57E-01	6.94E-02	0.73
CS	2.57E-01	9.90E-02	7.58E-01	1.20E-01	2.15

Table 6. Same as Table 5, but for each rupture rather than each segment, and total aggregated probabilities for each fault are included here as well.

Rupture Name	BPT Wt Ave with α constant	BPT Min with α constant	BPT Max with α constant	Pois Wt Ave	BPT Gain
Elsinore					
W	1.18E-02	4.54E-03	3.98E-02	4.66E-03	2.53
GI	3.77E-03	2.25E-11	1.16E-02	1.05E-02	0.36
T	1.81E-03	3.69E-07	4.03E-03	2.10E-03	0.86
J	1.79E-04	0.00E+00	7.20E-04	7.91E-05	2.27
CM	1.11E-03	0.00E+00	8.45E-03	5.34E-03	0.21
W+GI	2.85E-04	0.00E+00	1.85E-03	2.09E-04	1.36
GI+T	1.92E-03	2.27E-07	5.16E-03	2.52E-03	0.76
T+J	5.26E-04	0.00E+00	1.63E-03	3.15E-04	1.67
J+CM	1.06E-03	0.00E+00	4.24E-03	5.82E-04	1.81
W+GI+T	1.30E-04	0.00E+00	6.34E-04	1.44E-04	0.90
GI+T+J	4.47E-04	0.00E+00	1.36E-03	3.15E-04	1.42
T+J+CM	1.47E-03	5.57E-04	3.03E-03	1.30E-03	1.13
W+GI+T+J	9.74E-05	0.00E+00	3.19E-04	6.24E-05	1.56
GI+T+J+CM	9.65E-04	4.75E-04	1.68E-03	1.02E-03	0.95
W+GI+T+J+CM	8.72E-05	0.00E+00	2.84E-04	6.26E-05	1.39
Total Probability	2.54E-02	1.50E-02	5.39E-02	2.89E-02	0.88
Garlock					
GE	6.32E-03	2.65E-03	1.26E-02	2.92E-03	2.16
GC	3.88E-04	5.74E-06	6.70E-04	4.16E-04	0.93
GW	5.65E-04	2.18E-07	1.48E-03	1.19E-03	0.47
GE+GC	4.60E-04	1.88E-04	6.72E-04	4.14E-04	1.11
GC+GW	1.78E-03	1.25E-05	3.90E-03	2.22E-03	0.80
GE+GC+GW	2.05E-03	4.26E-04	3.86E-03	2.23E-03	0.92
Total Probability	1.15E-02	8.12E-03	1.59E-02	9.37E-03	1.23
San Jacinto					
SBV	1.46E-02	4.51E-04	3.83E-02	7.54E-03	1.93
SJV	4.95E-03	1.55E-06	1.38E-02	7.66E-03	0.65

A	3.80E-04	0.00E+00	1.34E-03	2.20E-04	1.72
C	1.83E-04	0.00E+00	6.20E-04	2.23E-04	0.82
CC	9.81E-04	1.05E-07	3.54E-03	3.36E-03	0.29
B	4.17E-03	0.00E+00	1.81E-02	1.30E-02	0.32
SM	2.35E-02	7.95E-03	1.00E-01	9.57E-03	2.46
SBV+SJV	4.52E-03	1.09E-04	9.28E-03	4.48E-03	1.01
SJV+A	1.40E-03	0.00E+00	4.59E-03	1.11E-03	1.26
A+C	1.87E-02	3.50E-03	3.85E-02	1.09E-02	1.72
A+CC	3.36E-04	0.00E+00	1.21E-03	2.23E-04	1.51
CC+B	9.05E-04	6.59E-08	3.48E-03	3.36E-03	0.27
B+SM	4.99E-03	1.54E-03	1.13E-02	3.81E-03	1.31
SBV+SJV+A	1.38E-03	0.00E+00	4.94E-03	1.12E-03	1.24
SJV+A+C	1.27E-03	0.00E+00	3.93E-03	1.12E-03	1.13
SJV+A+CC	2.58E-04	0.00E+00	8.40E-04	2.23E-04	1.16
A+CC+B	3.14E-04	0.00E+00	1.14E-03	2.25E-04	1.40
CC+B+SM	2.80E-03	1.33E-03	5.06E-03	3.33E-03	0.84
SBV+SJV+A+C	5.46E-03	1.51E-03	1.11E-02	3.73E-03	1.46
SBV+SJV+A+CC	2.58E-04	0.00E+00	9.32E-04	2.24E-04	1.15
SJV+A+CC+B	2.42E-04	0.00E+00	7.99E-04	2.21E-04	1.10
A+CC+B+SM	3.30E-04	0.00E+00	1.20E-03	2.24E-04	1.48
SBV+SJV+A+CC+B	2.43E-04	0.00E+00	8.92E-04	2.22E-04	1.09
SJV+A+CC+B+SM	2.62E-04	0.00E+00	8.74E-04	2.25E-04	1.17
SBV+SJV+A+CC+B+SM	2.56E-04	0.00E+00	9.24E-04	2.21E-04	1.16
Total Probability	8.90E-02	4.28E-02	1.86E-01	7.38E-02	1.21
N. San Andreas					
SAO	3.25E-03	3.38E-04	7.33E-03	3.94E-03	0.83
SAN	6.04E-05	8.10E-07	1.17E-04	1.02E-04	0.59
SAP	1.15E-03	2.80E-06	3.22E-03	1.50E-03	0.77
SAS	8.24E-03	7.40E-04	1.69E-02	7.49E-03	1.10
SAO+SAN	6.59E-03	4.83E-04	1.59E-02	9.81E-03	0.67
SAN+SAP	2.78E-06	0.00E+00	1.06E-05	5.24E-06	0.53
SAP+SAS	8.28E-03	8.89E-04	2.21E-02	9.80E-03	0.84
SAO+SAN+SAP	2.46E-04	1.25E-05	4.71E-04	3.55E-04	0.69
SAN+SAP+SAS	8.21E-05	1.14E-05	1.46E-04	1.20E-04	0.68
SAO+SAN+SAP+SAS	6.47E-03	2.63E-04	1.68E-02	8.74E-03	0.74

Total Probability	3.38E-02	4.54E-03	6.05E-02	4.12E-02	0.82
S. San Andreas					
PK	4.16E-02	1.66E-06	1.92E-01	1.66E-01	0.25
CH	5.59E-04	3.64E-04	1.16E-03	2.58E-04	2.17
CC	1.91E-03	3.91E-04	4.19E-03	1.02E-03	1.87
BB	3.69E-03	2.23E-03	6.72E-03	2.11E-03	1.75
NM	1.42E-03	4.78E-04	2.81E-03	8.24E-04	1.72
SM	5.38E-03	2.68E-03	9.61E-03	2.76E-03	1.95
NSB	8.26E-03	4.70E-03	2.57E-02	3.87E-03	2.14
SSB	4.32E-04	4.82E-05	7.48E-04	2.52E-04	1.72
BG	3.41E-03	7.53E-07	1.07E-02	1.56E-03	2.19
CO	7.21E-02	1.81E-02	3.16E-01	3.00E-02	2.40
PK+CH	3.73E-02	1.09E-02	1.36E-01	1.80E-02	2.07
CH+CC	2.60E-03	1.52E-03	4.42E-03	1.32E-03	1.97
CC+BB	2.14E-05	0.00E+00	5.88E-05	1.26E-05	1.69
BB+NM	4.00E-06	0.00E+00	1.03E-05	2.52E-06	1.59
NM+SM	3.68E-03	3.34E-05	1.16E-02	1.76E-03	2.09
SM+NSB	7.73E-03	4.48E-03	1.40E-02	3.96E-03	1.96
NSB+SSB	9.13E-03	4.37E-03	1.97E-02	4.70E-03	1.94
SSB+BG	4.93E-03	2.94E-06	1.63E-02	2.25E-03	2.19
BG+CO	6.49E-03	1.03E-03	1.61E-02	2.92E-03	2.22
PK+CH+CC	5.30E-03	2.88E-03	9.92E-03	2.80E-03	1.89
CH+CC+BB	4.67E-06	0.00E+00	1.42E-05	2.48E-06	1.88
CC+BB+NM	4.10E-06	0.00E+00	1.09E-05	2.52E-06	1.63
BB+NM+SM	2.18E-03	1.30E-03	3.72E-03	1.18E-03	1.84
NM+SM+NSB	8.48E-04	4.92E-04	1.67E-03	4.37E-04	1.94
SM+NSB+SSB	5.20E-03	3.02E-03	8.03E-03	2.73E-03	1.91
NSB+SSB+BG	2.58E-03	3.05E-05	7.19E-03	1.23E-03	2.09
SSB+BG+CO	2.99E-03	3.59E-04	7.87E-03	1.39E-03	2.15
PK+CH+CC+BB	5.60E-03	2.87E-03	1.16E-02	3.04E-03	1.84
CH+CC+BB+NM	4.48E-06	0.00E+00	1.30E-05	2.49E-06	1.80
CC+BB+NM+SM	2.41E-03	3.57E-05	5.83E-03	1.24E-03	1.94
BB+NM+SM+NSB	4.29E-06	0.00E+00	1.18E-05	2.50E-06	1.72
NM+SM+NSB+SSB	1.52E-03	6.17E-04	3.28E-03	7.78E-04	1.95
SM+NSB+SSB+BG	2.56E-03	7.56E-04	5.33E-03	1.29E-03	1.99

NSB+SSB+BG+CO	3.16E-03	3.15E-05	7.64E-03	1.47E-03	2.14
PK+CH+CC+BB+NM	1.05E-02	5.06E-03	2.22E-02	5.84E-03	1.80
CH+CC+BB+NM+SM	3.96E-03	1.12E-03	7.44E-03	2.06E-03	1.92
CC+BB+NM+SM+NSB	8.21E-04	4.11E-04	1.47E-03	4.37E-04	1.88
BB+NM+SM+NSB+SSB	4.76E-04	3.53E-04	7.57E-04	2.57E-04	1.85
NM+SM+NSB+SSB+BG	7.21E-04	1.32E-04	1.70E-03	3.63E-04	1.98
SM+NSB+SSB+BG+CO	3.78E-03	1.18E-03	7.37E-03	1.86E-03	2.03
PK+CH+CC+BB+NM+SM	1.30E-02	3.55E-05	2.93E-02	6.75E-03	1.92
CH+CC+BB+NM+SM+NSB	4.49E-06	0.00E+00	1.31E-05	2.48E-06	1.81
CC+BB+NM+SM+NSB+SSB	8.56E-04	4.41E-04	1.49E-03	4.59E-04	1.86
BB+NM+SM+NSB+SSB+BG	4.21E-06	0.00E+00	1.15E-05	2.52E-06	1.67
NM+SM+NSB+SSB+BG+CO	7.58E-04	1.06E-04	1.78E-03	3.72E-04	2.04
PK+CH+CC+BB+NM+SM+NSB	4.68E-03	2.53E-03	8.89E-03	2.50E-03	1.87
CH+CC+BB+NM+SM+NSB+SSB	4.82E-04	3.55E-04	7.48E-04	2.55E-04	1.89
CC+BB+NM+SM+NSB+SSB+BG	4.11E-04	1.80E-04	7.68E-04	2.19E-04	1.88
BB+NM+SM+NSB+SSB+BG+CO	4.62E-04	2.81E-04	8.23E-04	2.40E-04	1.92
PK+CH+CC+BB+NM+SM+NSB+SSB	9.77E-04	7.02E-04	1.48E-03	5.25E-04	1.86
CH+CC+BB+NM+SM+NSB+SSB+BG	4.43E-06	0.00E+00	1.27E-05	2.50E-06	1.77
CC+BB+NM+SM+NSB+SSB+BG+CO	9.22E-05	6.37E-05	1.58E-04	4.86E-05	1.90
PK+CH+CC+BB+NM+SM+NSB+SSB+BG	4.39E-04	2.52E-04	7.54E-04	2.34E-04	1.88
CH+CC+BB+NM+SM+NSB+SSB+BG+CO	4.56E-06	0.00E+00	1.40E-05	2.50E-06	1.82
PK+CH+CC+BB+NM+SM+NSB+SSB+BG+CO	8.41E-04	2.29E-04	1.57E-03	4.37E-04	1.93
Total Probability	2.53E-01	1.68E-01	5.01E-01	2.59E-01	0.98
Hayward-Rogers Creek					
RC	4.62E-02	1.99E-02	1.12E-01	2.05E-02	2.25
HN	4.23E-02	1.97E-02	1.02E-01	1.73E-02	2.45
HS	3.48E-02	1.36E-02	8.20E-02	1.85E-02	1.88
RC+HN	5.83E-03	3.43E-03	1.26E-02	2.59E-03	2.25
HN+HS	2.83E-02	1.01E-02	8.08E-02	1.32E-02	2.14
RC+HN+HS	3.38E-03	2.00E-03	7.58E-03	1.58E-03	2.14
Total Probability	1.49E-01	7.32E-02	3.41E-01	7.15E-02	2.09
Calaveras					
CN	1.03E-02	9.29E-04	4.19E-02	7.05E-03	1.47
CC	3.16E-02	6.89E-05	9.58E-02	4.46E-02	0.71

CS	2.05E-01	7.44E-02	6.23E-01	9.71E-02	2.11
CN+CC	6.74E-04	6.44E-05	1.92E-03	6.86E-04	0.98
CC+CS	1.84E-02	7.87E-03	4.40E-02	1.83E-02	1.01
CN+CC+CS	9.53E-03	2.36E-03	3.55E-02	7.38E-03	1.29
Total Probability	2.53E-01	1.20E-01	6.91E-01	1.64E-01	1.54